ISBN: 978-3-95450-225-7 ISSN: 2673-5571 doi:10.18429/JACoW-HB2021-MOP17

END-TO-END LONGITUDINAL SIMULATIONS IN THE CERN PS

A. Lasheen*, H. Damerau, K. Iliakis, CERN, Geneva, Switzerland

Abstract

In the context of the LHC Injector Upgrade (LIU) project, the main longitudinal limitations in the CERN PS are coupled bunch instabilities and uncontrolled emittance blow-up leading to losses at injection into the downstream accelerator, the SPS. To complement beam measurements, particle tracking simulations are an important tool to study these limitations. However, to avoid excessive runtime, simulations are usually targeting only a fraction of the cycle assuming that bunches are initially matched to the RF bucket. This ignores all initial perturbations that could seed an instability. Simulations were therefore performed along the full PS cycle by using the BLonD tracking code optimized with advanced parallelization schemes. They include beam manipulations with several RF harmonics (batch compression, merging, splittings), controlled emittance blow-up, a model of the beam coupling impedance covering a wide frequency range, as well as beam and cavity feedbacks. A large number of macroparticles is required as well as arrays to store beam induced voltage spanning several revolutions to account for long range wakefields.

INTRODUCTION

The main target of the High Luminosity (HL)-LHC project is to increase the luminosity for collisions by an order of magnitude [1]. This objective relies on an increased beam brightness from the injectors, which were upgraded in the framework of the LHC Injector Upgrade (LIU) project [2]. The beam intensity shall be doubled. However, at high beam current, limitations arise due to collective effects such as beam instabilities or uncontrolled emittance blow-up.

In the PS, the two main longitudinal limitations to reach the target of $N_b = 2.6 \times 10^{11}$ protons per bunch (p/b) at extraction are coupled bunch instabilities along the ramp (dipolar and quadrupolar) as well as uncontrolled longitudinal emittance blow-up due to high frequency cavity impedance [3, 4]. The longitudinal emittance should be kept at the nominal value of $\varepsilon_l = 0.35$ eVs at extraction to fit in the rf bucket of the SPS, the final stage in the LHC injector chain. Therefore, extensive studies were conducted to find means to mitigate beam instabilities.

An essential tool for beam instability studies are macroparticle simulations. Previously the simulations were done targeting only a specific instance in the cycle to keep the runtime reasonable (hours to couple of days). An example is the study of dipolar coupled bunch instabilities where simulations were initially performed at constant beam energy [5]. The initial particle distribution then needs to be assumed as matched to the initial RF bucket or with an arbitrary mismatch. In reality mismatches accumulate all along the cycle and can seed the onset of an instability. They should therefore be taken into account to better reproduce the instability threshold. For example, coupled bunch instabilities start after transition crossing where an initial perturbation is expected, while simulations were originally started with matched conditions during the ramp.

Several studies could benefit from tracking simulations covering a complete cycle. An example is the operation with a higher harmonic RF cavity as Landau RF system to damp instabilities [6]. The present option consists of using the narrow-band 40 MHz cavity along the ramp. However, due to the limited bandwidth of the system, the complete acceleration ramp cannot be covered in such an operation mode. Tracking simulations covering the whole ramp, including transition crossing, were hence needed to evaluate the necessity of a dedicated Landau RF system.

Another aspect is the generation of particles at large amplitude in the longitudinal phase space (referred to as "longitudinal halo"), beyond the 0.35 eVs amplitude at extraction which are lost at SPS injection. The generation of halo can occur at several stages during the cycle and may accumulate. The optimization of the bunch rotation prior to extraction then requires a good knowledge of the halo. A simulation covering the whole cycle is needed to evaluate the impact of each stage in the cycle in terms of halo generation.

In this paper, the particle tracking code BLonD was extended in order to take into account several aspects such as a dynamic beam coupling impedance model, the influence of feedback systems, as well as a complete representation of the cycle including all processes and RF manipulations. The simulation is then compared to measurements. Finally, the computing performances are detailed.

MODELING THE COMPLETE ACCELERATION CYCLE

Beams with various longitudinal parameters can be generated in the PS. In the context of this paper, the so-called BCMS-type beam (Batch Compression Merging Splitting) produced for the LHC is considered [7]. The complete momentum and RF voltage programs are shown in Fig. 1. In this configuration, 8 bunches are injected from the PS Booster in two consecutive injections spaced by 1.2 s. The beam is then accelerated to an intermediate energy plateau where RF manipulations are performed. The beam is thereafter accelerated to the top energy, passing through transition crossing. The beam is then split again four times and non-adiabatically shortened before extraction to fit in the 5 ns SPS RF bucket (bunch rotation). Along the cycle, the longitudinal emittance is adjusted by applying controlled blow-up [8].

The complete program was simulated using the BLonD tracking code [9] including all the RF manipulations and controlled blow-ups, with the same voltage programs as

* alexandre.lasheen@cern.ch

Content from this work may be used under the terms of the CC BY 3.0 licence (© 2021). Any distribution of this work must maintain attribution to the author(s), title of the work, publisher, and DOI

ISBN: 978-3-95450-225-7 ISSN: 2673-5571 doi:10.18429/JACoW-HB2021-MOP17

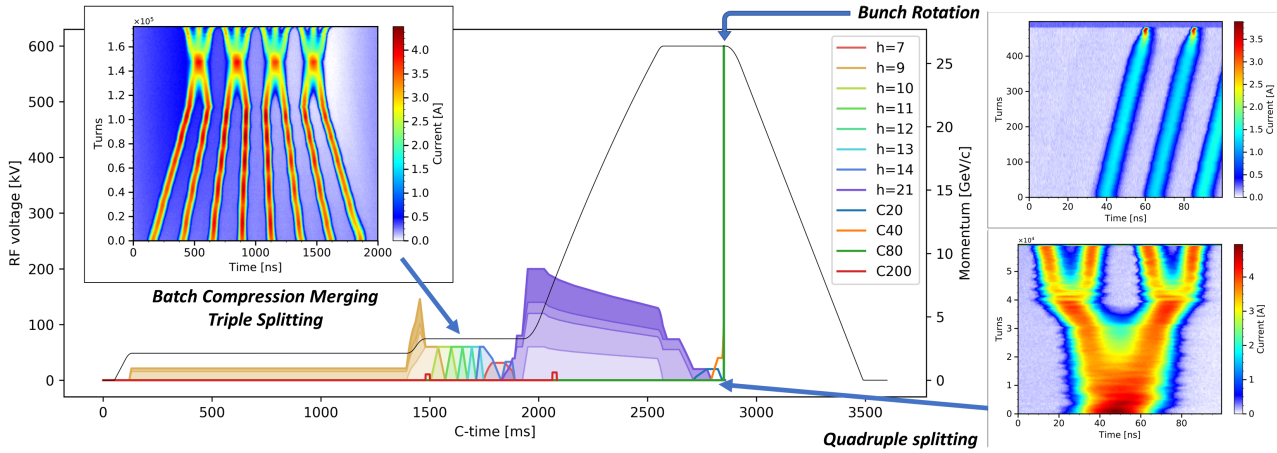

Figure 1: The momentum (black) and RF voltage program (colored) for the BCMS cycle. The RF harmonics h = 7 to 21 (10 MHz) are handled by tunable ferrite loaded cavities while the higher harmonics h = 42 (20 MHz), h = 84 (40 MHz) and h = 168 (80 MHz) are generated by fixed frequency RF systems. For each manipulation the evolution of the bunch profiles is shown.

set in the machine. A transition jump scheme is present in the PS [10]. In the simulation the evolution of γ_t was computed using the MAD-X code [11] and is included in the longitudinal simulation.

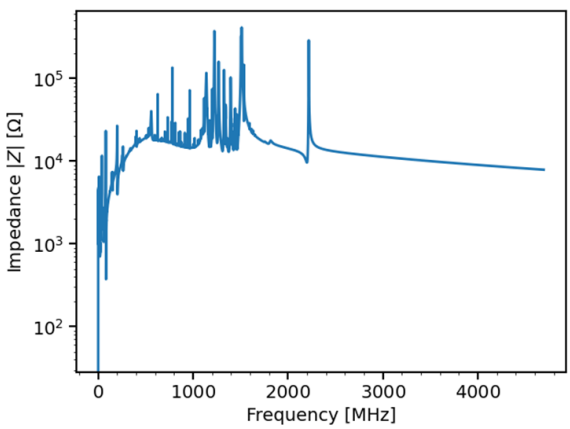

Figure 2: The PS impedance model. The contribution of vacuum equipment is visible at high frequency while the broadband component is due to the kickers.

The next step consisted of including intensity effects. The present PS beam coupling impedance model [12] used for simulations is the product of many years of development, and it now includes the impedance of the RF systems, injection and extraction elements (kickers, septa), vacuum equipment (flanges, pumping manifolds, sector valves), beam instrumentation, resistive wall impedance and longitudinal space charge. The impedance of the various elements are modeled using resonator functions or by passing the complete impedance table as obtained from electromagnetic simulations. While the model is continuously updated, the most important contributions are expected to be well represented. The absolute impedance model $|Z|(f)$ is displayed in Fig. 2.

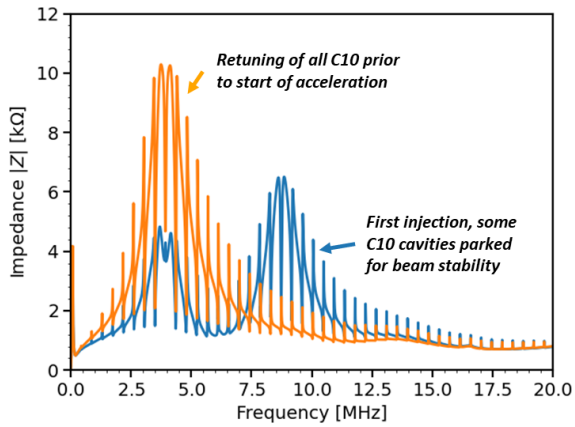

Figure 3: The impedance of the ten C10 cavities on the flat bottom energy and after second injection when accelerating to the intermediate plateau. The impedance is reduced by the OTDFB at revolution frequency harmonics except on the central frequency of the cavity when in use.

The impedance of the RF cavities require a specific treatment. Indeed, some of the cavities are tuned as the beam is accelerated and RF manipulations performed. The example for the accelerating tunable ferrite-loaded cavities (C10) is shown in Fig. 3. The impedance on the 1.2 s injection plateau is compared with the impedance at the start of acceleration. Additionally, each RF cavity is equipped with feedback systems to reduce beam loading. In the case of the C10 cavities, the impedance is reduced at multiples of the revolution frequency by a One Turn Delay Feedback (OTDFB) [13]. The parameters of the notches also need to be updated in simulations to follow the revolution frequency sweep. In the present implementation, the cavity impedance is treated in frequency domain and represented by

$$Z_{\mathrm{fb}}(\omega) = \frac{Z_c(\omega)}{1 + Z_c(\omega)\, GH(\omega)\, e^{j\omega\Delta t}}, \qquad (1)$$

Content from this work may be used under the terms of the CC BY 3.0 licence (© 2021). Any distribution of this work must maintain attribution to the author(s), title of the work, publisher, and DOI

ISBN: 978-3-95450-225-7 ISSN: 2673-5571 doi:10.18429/JACoW-HB2021-MOP17

Content from this work may be used under the terms of the CC BY 3.0 licence (© 2021). Any distribution of this work must maintain attribution to the author(s), title of the work, publisher, and DOI

where Z_c is the cavity impedance including direct feedback obtained from beam based measurements [14], $H(\omega)$ the transfer function of the OTDFB comb filter centered at revolution frequency harmonics, Δt the loop delay and G the feedback gain.

For narrowband impedance sources or long delay cavity feedback systems, the decay of the induced voltage can span over many revolution periods. In order to include transient effects with non-stationary beams, a multi-turn induced voltage algorithm was included in BLonD. An example is presented in Fig. 4. The algorithm relies on computing the induced voltage as a large array covering many turns, sufficient to have a complete decay of the signal (150 turns in the present simulation). The second half of the array is set to zero to avoid unphysical artefacts due to the circular convolution (75 effective turns). The induced voltage at a given turn is computed from a circular convolution of the beam current multiplied to the impedance, using Fast Fourier Transforms (FFTs). The contribution from the previous turns, kept in the memory, is then added to the induced voltage to get the total induced voltage. Note that the present treatment of cavity feedback systems by a direct modification of the transfer function do not include potential power limitations. This would require to decompose the signal processing chain.

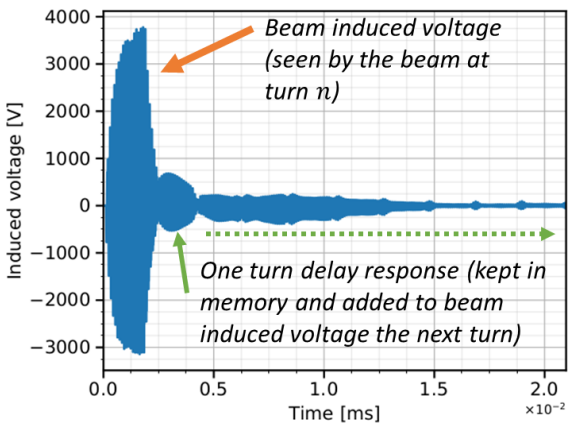

Figure 4: The induced voltage of the C10 cavities including OTDFB on a time period covering ten turns. The impulse response of the feedback is kept in the memory and added to the following simulated turns.

Another intensity effect to consider is longitudinal space charge, which is dominant at low energy in the PS and gradually becomes negligible during acceleration. The evolution of space charge treated as a pure reactive impedance is shown in Fig. 5. The present treatment uses the classical representation of longitudinal space charge with

$$\left(\frac{Z}{n}\right)_{\mathrm{sc}} = -j\frac{Z_0}{\beta\gamma^2}g, \tag{2}$$

where $n = \omega/\omega_0$ is the ratio to the revolution frequency ω_0, Z_0 is the vacuum impedance, β, γ are the relativistic velocity and mass factors that evolve during the ramp, and g a geometric factor depending on the transverse beam size and the aperture geometry. The value of $(Z/n)_{\mathrm{sc}}$ is updated each turn during the simulation accounting for the evolution of the beam energy and transverse size (via transverse emittance and momentum spread δ). A more advanced model of longitudinal space charge including the influence of the motion of single particles in the transverse plane for the PS is presently developed in [15].

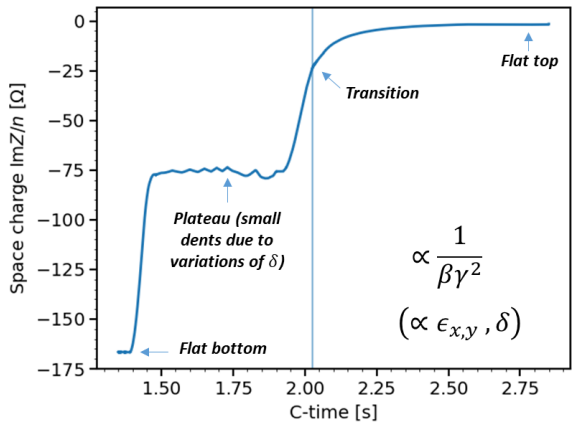

Figure 5: Longitudinal space charge impedance along the cycle, including the variations in energy and transverse beam size. The optics is assumed to remain unchanged during acceleration.

Finally, simplified beam control loops were also included in the simulation using the BLonD implementation as baseline [16]. The beam is accelerated using a phase loop to mitigate zero mode bunch phase oscillations, while the slow drifts in orbit (and consequently in RF frequency) are reduced by a radial loop. The gains were adjusted empirically to obtain stable beam loops and implemented as simple proportional and integrator corrections with

$$\Delta\omega_{\mathrm{PL},i} = -g_{\mathrm{PL}}\Delta\phi_i, \tag{3}$$

$$\Delta\omega_{\mathrm{RL},i} = \Delta\omega_{\mathrm{RL},i-1} - \mathrm{sgn}(\eta)\, g_{\mathrm{RL}}\left(\frac{\Delta R}{R}\right)_i, \tag{4}$$

where the loop corrections on the RF frequency $\Delta\omega$ are summed and applied each turn i, resulting in a variation in RF phase at the next turn $i+1$. The beam phase error $\Delta\phi$ is obtained by a convolution with the instantaneous RF waveform (including its variation in frequency each turn), while the orbit error ΔR is obtained by taking the mean macro-particle offset in energy with respect to the design energy, converted into an orbit via the momentum compaction factor. The gains $g_{\mathrm{PL}}, g_{\mathrm{RL}}$ were adjusted to keep the phase loop action in a time scale much smaller than the one of the radial loop (respectively few μs versus ms). The sign of the radial loop correction is flipped at transition crossing with the sign of the phase slippage factor η. An extraction synchronization loop was also included at top energy like in the machine, in the same form as the phase loop Eq. (3). In this case however the phase is compared with a signal at fixed frequency corresponding to the expected $h = 1$. The radial loop is disabled once the synchronization loop

ISBN: 978-3-95450-225-7 ISSN: 2673-5571 doi:10.18429/JACoW-HB2021-MOP17

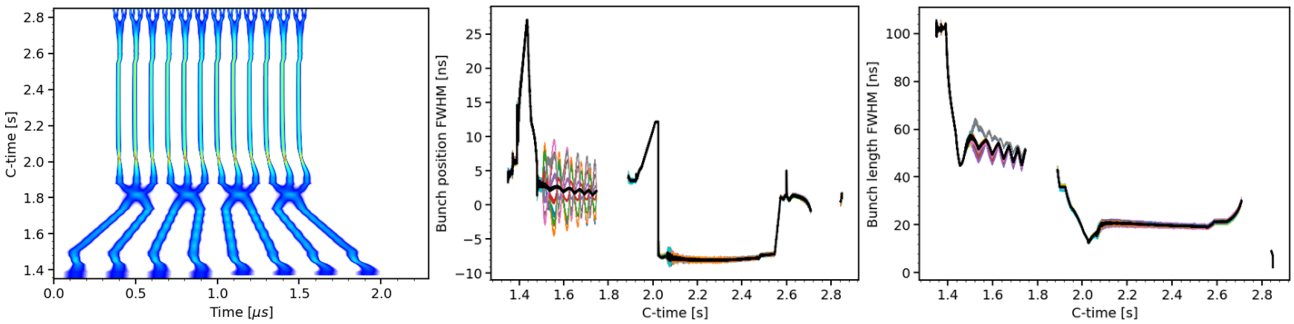

Figure 6: The complete simulated BCMS cycle. The beam profile (left) is shown all along the cycle, including both injections, acceleration to the intermediate plateau, batch compression, merging, splitting, acceleration, transition crossing, controlled emittance blow-up, double splittings, bunch rotation. The bunch-by-bunch position (or phase, middle) and length (right) is analyzed to monitor the evolution of the bunch parameters and identify potential instabilities (colored traces are bunch-by-bunch, black is average). Bunch length and position are not computed during the splittings leading to the blank areas in the corresponding plots.

is enabled. The present model of the beam control loops implies that the phase and radial loops are DC-coupled and act upon the same bandwidth, which is not the case in the machine (AC-coupled phase loop). Although sufficient in simulations, a more realistic implementation is necessary to fully reproduce the dynamic behavior, for instance close to transition crossing.

SIMULATED CYCLE AND COMPARISON WITH MEASUREMENTS

The elements described in the previous section were assembled to perform a complete simulation including the full RF program, intensity effects as well as feedback systems. The result is detailed in Fig. 6. The beam profile as it would be measured by a Wall Current Monitor is saved regularly along the simulation to monitor its evolution. The RF manipulations introduced in Fig. 1 are well reproduced. Note that the relative phase of the RF systems were adjusted to minimize the bunch-by-bunch spread in intensity and longitudinal emittance at extraction, just as it is done in real operation. To do so, the simulation parameters such as the longitudinal distribution are saved at each stage of the simulated cycle to optimize sequentially the parameters of the RF manipulations. This is necessary as transient beam loading will induce phase shifts as a function of the beam intensity.

For each simulated beam profile, the bunch positions and lengths are obtained from the Full Width Half Maximum (FWHM). They can then be compared with measurements or used to identify the onset of an instability. The bunch positions (Fig. 6, middle) are expressed with respect to zero crossing of the RF waveform. Hence, the obtained curve follows the synchronous phase evolution along the cycle, with a phase jump at transition crossing. Note that due to beam loading the mean position is shifted due to the resitive impedance (synchronous phase shift). The glitch at the cycle time about 2.6 s is due to the synchronization

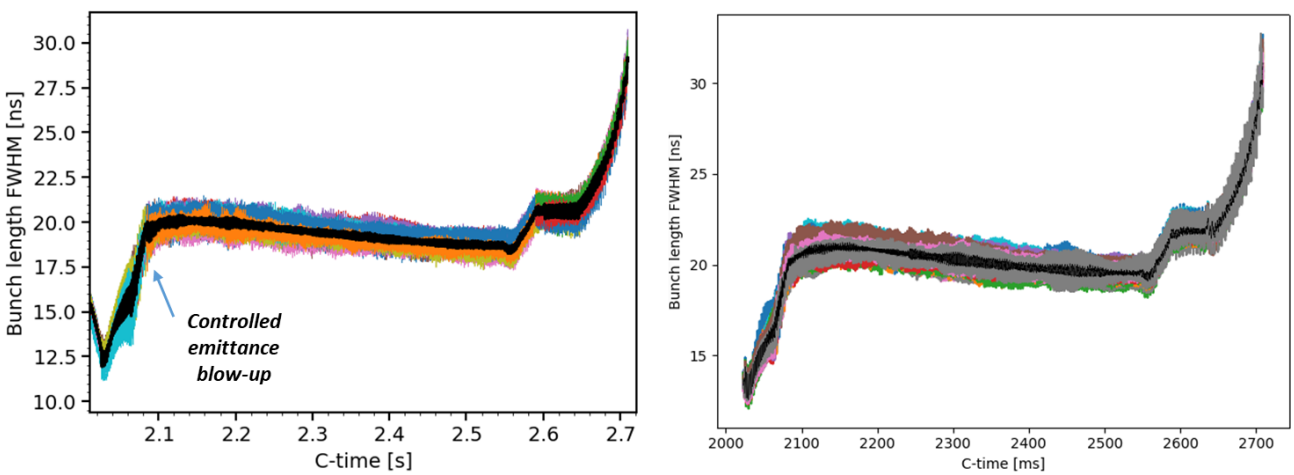

Figure 7: Simulated (left) and measured (right) bunch lengths along the acceleration ramp starting right before transition crossing until the double splittings at flat top energy. The bunch-by-bunch lengths are represented in colors while the mean value is shown in black.

Content from this work may be used under the terms of the CC BY 3.0 licence (© 2021). Any distribution of this work must maintain attribution to the author(s), title of the work, publisher, and DOI

ISBN: 978-3-95450-225-7 ISSN: 2673-5571 doi:10.18429/JACoW-HB2021-MOP17

Content from this work may be used under the terms of the CC BY 3.0 licence (© 2021). Any distribution of this work must maintain attribution to the author(s), title of the work, publisher, and DOI

loop. The bunch lengths along the cycle are displayed in the right plot in Fig. 6. The variation of the bunch length τ_l from injection to extraction covers almost 2 orders of magnitude. This is an essential parameter regarding intensity effects (e.g. space charge induced voltage scales with $1/\tau_l^3$). Additionally, this is also important for numerical noise and the choice of the number of macroparticles which impacts the simulation runtime. The numerical noise is increased for longer bunches with a fixed number of macroparticles and bin size for the induced voltage calculation.

The simulated and measured bunch length evolution are compared in Fig. 7. To reach this agreement, the RF voltage used for controlled emittance blow-up had to be increased by about a factor two with respect to the expected value. Although the effective RF voltage in the 200 MHz cavities is not known precisely, further investigations are ongoing to find the source of the discrepancy. Nonetheless, after adjusting the voltage applied for the blow-up, the evolution of the bunch length along the ramp until the last splittings is in excellent agreement with the measurements. After bunch rotation, the bunch length at extration is about 4 ns which is also in perfect agreement with the expectations in real operation. Overall, the measurements for a stable beam are well reproduced in simulations.

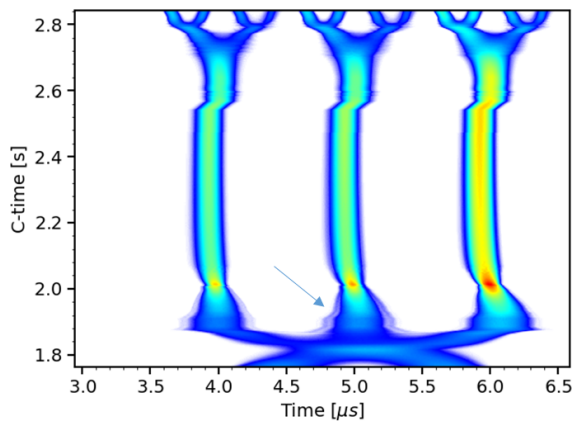

Figure 8: Example of beam profile evolution including a mismatch during the handover between the phase loop from $h = 7$ to $h = 21$ after the triple splitting. It generates particles at large amplitude in the RF bucket which are preserved all along the acceleration cycle and kept until top energy.

The benchmark of the model should be completed to calibrate gains of the feedack systems and identify possibly missing impedance sources. Nonetheless, simulations already provide interesting features to analyze, comparable to real operation. An example is presented in Fig. 8. During RF manipulations, the phase discrimination for the phase loop needs to be switched when changing the main RF harmonic. In the context of the triple splitting, the phase loop is handed over from the RF harmonic $h = 7$ to $h = 21$. The initial offset at $h = 21$ needs then to be adjusted to start with zero phase loop error, minimizing the transient of the loop. However, an error in the phase loop offset can lead to beam oscillations that will be quickly damped but nonetheless contribute to populate particles at large amplitude in the RF bucket. As shown in Fig. 8 these particles will be kept until the flat top, and eventually contribute to the losses at SPS injection. The present acquisition systems make the measurement of the longitudinal halo generation along the cycle very difficult. This effect can now be studied in simulation by adding all potential sources of halo generation.

To make the simulation possible in a reasonable time frame, the BLonD simulation code was optimized and parallelized combining OpenMP and MPI [17, 18]. The example from the previous section was made sampling the complete impedance model up to 5 GHz, using 480 M macroparticles to have sufficiently low numerical noise for the induced voltage calculation. The runtime was of the order of 2.5 days using 4 MPI nodes with 20 cores each and could be further reduced increasing the number of nodes. The repartition for the different numerical routines is listed in the table below.

Numerical routine	Runtime %
Induced voltage FFTs	50%
Tracking (including beam loops)	20%
Beam profile update	13%
Space charge update	7%
Impedance update	5%
Other (plots...)	5%

The present bottleneck in computing time is the induced voltage calculation due to the FFTs with large numbers of points. Although several approaches could be considered to reduce this runtime (e.g. time domain modeling of the feedback systems, adapting bin size depending to the bunch length to neglect very high frequency impedance sources), it appears that the present level of optimization is sufficient to cover a frequency range including all possible resonances and yet keep the simulation runtime in the order of days.

CONCLUSIONS

The complete BCMS cycle of the PS was modeled including RF manipulations, intensity effects (impedance model and space charge) as well as feedback systems (cavity and beam loops). The initial results show that the main features of the cycle are well reproduced and are comparable to the observations. A complete benchmark campaign is needed to adjust the parameters that were set empirically such as the feedback gains. The model can then be used to simulate beam instabilities and include remaining items such as the coupled-bunch feedback. The optimization of the BLonD code through large scale parallelization allows the simulation of the full cycle while keeping the runtime in the order of days. This opens the door to instability studies including all sources of initial perturbations, low and high frequency impedance sources and tracking of the longitudinal halo along the cycle.

ACKNOWLEDGMENTS

The authors would like to thank the BLonD developer team, as well as all contributors to the PS impedance model.

ISBN: 978-3-95450-225-7 ISSN: 2673-5571 doi:10.18429/JACoW-HB2021-MOP17

REFERENCES

[1] "High-Luminosity Large Hadron Collider (HL-LHC): Technical design report," Tech. Rep. CERN-2020-010, Geneva, 2020.

[2] J. Coupard, H. Damerau, A. Funken, R. Garoby, S. Gilardoni, B. Goddard, K. Hanke, A. Lombardi, D. Manglunki, M. Meddahi, B. Mikulec, G. Rumolo, E. Shaposhnikova, and M. Vretenar, "LHC Injectors Upgrade, Technical Design Report," Tech. Rep. CERN-ACC-2014-0337, 2014.

[3] H. Damerau, S. Hancock, C. Rossi, E. Shaposhnikova, J. Tuckmantel, J.-L. Vallet, and M. Mehler, "Longitudinal Coupled-Bunch Instabilities in the CERN PS", in *Proc. 22nd Particle Accelerator Conf. (PAC'07)*, Albuquerque, NM, USA, Jun. 2007, paper FRPMN069, pp. 4180–4182.

[4] H. Damerau and L. Ventura, "Longitudinal coupled-bunch instability studies in the PS," in *Injector MD Days 2017*, no. CERN-Proceedings-2017-002, pp. 59–62, 2017.

[5] L. Ventura, "Studies of Longitudinal Coupled-Bunch Instabilities in the LHC Injectors Chain", Ph.D. thesis, Rome U., Rome, Italy, 2017.

[6] H. Damerau, A. Lasheen, and E. N. Shaposhnikova, "Higher-Harmonic RF System for Landau Damping in the CERN PS", in *Proc. 9th Int. Particle Accelerator Conf. (IPAC'18)*, Vancouver, Canada, Apr.-May 2018, pp. 728–731. doi:10.18429/JACoW-IPAC2018-TUPAF026

[7] H. Damerau, H. Bartosik, R. Garoby, S. Gilardoni, S. Hancock, B. Mikulec, Y. Papaphilippou, G. Rumolo, E. Shaposhnikova, and R. Tomas, "LIU: exploring alternative ideas," in *RLIUP: Review of LHC and Injector Upgrade Plans*, pp. 127–137, 2014.

[8] H. Damerau, M. Morvillo, E. N. Shaposhnikova, J. Tuckmantel, and J.-L. Vallet, "Controlled Longitudinal Emittance Blow-up in the CERN PS", in *Proc. 22nd Particle Accelerator Conf. (PAC'07)*, Albuquerque, NM, USA, Jun. 2007, paper FRPMN070, pp. 4186–4188.

[9] "CERN Beam Longitudinal Dynamics code BLonD", https://blond.web.cern.ch/

[10] A. Sørensen, "Crossing The Phase Transition In Strong Focusing Proton synchrotrons," *Part. Accel.*, vol. 6, pp. 141–165, 1975.

[11] "MAD - Methodical Accelerator Design", http://madx.web.cern.ch/madx/

[12] "PS Longitudinal Impedance Model (2019)", Zenodo, 2020. doi:10.5281/zenodo.4722835

[13] F. Blas and R. Garoby, "Design and operational results of a "one-turn-delay feedback" for beam loading compensation of the CERN PS ferrite cavities," Tech. Rep. CERN-PS-91-16-RF, May 1991.

[14] G. Favia, "Study of the beam-cavity interaction in the CERN PS 10 MHz cavities and investigation of hardware solutions to reduce beam loading,"Ph.D. Thesis, Univ. of Rome, Rome, Italy, 2017.

[15] A. Laut and A. Lasheen, "Influence of Transverse Motion on Longitudinal Space-Charge in the CERN PS," this conference.

[16] H. Timko, J. E. Müller, A. Lasheen, and D. Quartullo, "Benchmarking the Beam Longitudinal Dynamics Code BLonD", in *Proc. 7th Int. Particle Accelerator Conf. (IPAC'16)*, Busan, Korea, May 2016, pp. 3094–3097. doi:10.18429/JACoW-IPAC2016-WEPOY045

[17] K. Iliakis, H. Timko, S. Xydis, and D. Soudris, "Blond++: Performance analysis and optimizations for enabling complex, accurate and fast beam dynamics studies," in *Proceedings of the 18th International Conference on Embedded Computer Systems: Architectures, Modeling, and Simulation*, SAMOS '18, (New York, NY, USA), p. 123-30, Association for Computing Machinery, 2018.

[18] K. Iliakis, H. Timko, S. Xydis, and D. Soudris, "Scale-out beam longitudinal dynamics simulations," in *Proceedings of the 17th ACM International Conference on Computing Frontiers*, CF '20, (New York, NY, USA), p. 29-38, Association for Computing Machinery, 2020.

Content from this work may be used under the terms of the CC BY 3.0 licence (© 2021). Any distribution of this work must maintain attribution to the author(s), title of the work, publisher, and DOI